CrystEngComm

Accepted Manuscript

ROYAL SOCIETY OF CHEMISTRY

www.rsc.org/crystengcomm

Cite this: DOI: 10.1039/c0xx00000x

www.rsc.org/xxxxxx

ARTICLE TYPE

Microstructure of epitaxial film of anatase nanotubes obtained at high voltage and mechanism of its electrochemical reaction with sodium

José R. González, Ricardo Alcántara*, Francisco Nacimiento, Gregorio F. Ortiz and José L. Tirado

Received (in XXX, XXX) Xth XXXXXXXXX 20XX, Accepted Xth XXXXXXXXX 20XX

DOI: 10.1039/b000000x

Titania nanotubes (nt-TiO_2) with high aspect ratio and amorphous character have been prepared by Ti anodization at high voltage (100 V). After annealing, the nanotubes crystallize to anatase phase and the XRD patterns and TEM images show that self-organized anatase nt-TiO_2 are composed of crystallographically oriented nanocrystalline domains on Ti substrate. The contribution of faradic and pseudocapacitive processes is studied for anatase nt-TiO_2 in Na cells obtaining the b-parameter from cyclic voltammetry experiments. The reaction between anatase nt-TiO_2 and Na is dominated by redox surface processes (pseudocapacitance) in the region over ca. 0.5 V and by irreversible faradic processes below ca. 0.3 V. The cycling performance of anatase nt-TiO_2 in sodium cell is very strongly affected by the imposed electrochemical conditions. Reversible capacity values of about 150-200 mAh g^{-1} and good cycling behaviour are found for 2.6-0.5 V of potential limits. Impedance spectra and ^{23}Na MAS NMR spectra are also used to study the reactions mechanisms. In addition, it is found that using variable voltage during the anodization of titanium, the resulting electrode exhibits excellent cycling behaviour (ca. 190 mAh g^{-1} after ca. 800 cycles). These results are the best cycling behaviour reported to date for anatase in the form of self-organized nanotubes for sodium ion microbatteries.

1. Introduction

Titanium dioxide is among the materials regarded as very promising candidates to replace carbon as negative electrode of lithium ion batteries.[1-4] Titanium dioxide can be prepared amorphous or in crystalline forms. The relevant polymorphic forms of TiO_2 for lithium batteries are rutile, anatase, brookite and TiO_2(B). Anatase possesses relatively high capacity for lithium insertion into its structure (theoretically up to stoichiometry $LiTiO_2$). The lithium ions can be inserted without largely distorting the anatase structure. The nanosizing of titanium dioxide, for example in the form of nanotubes prepared by anodization of Ti,[3-5] can increase its capacity to store lithium. This feature may be related to shorter diffusion path length of lithium ions, increase of the electronic conductivity and storage of lithium ions in the titania nanoparticle surface. On the other hand, the theoretical maximum volumetric capacity ($LiTiO_2$, for anatase 1297 mAh cm^{-3} and 1440 for rutile, 1307 mAh cm^{-3}) is higher than that of graphite (837 mAh cm^{-3} for LiC_6).[6]

Bonino et al.[7] and Ohzuku et al.[8] first reported ex-situ XRD data of anatase electrochemically reduced in lithium cell where firstly the reflections of anatase are preserved and after further lithium insertion the tetragonal lattice is transformed into a orthorhombic unit cell. Several diffraction, XPS, ^{7}Li NMR, X-ray absorption spectrocopy and Raman spectroscopy studies have confirmed that the mechanism of lithium insertion/removal into anatase follows a reversible two-phase transition process:[9]

TiO_2 ($I4_1/amd$) → $Li_{0.5}TiO_2$ (*Imma*) → $LiTiO_2$ ($I4_1/amd$)

The occurrence of the gamma phase ($LiTiO_2$, s.g. $I4_1/amd$) is only observed in the case of nanosized titania. Besides lithium insertion capacity (faradic process), TiO_2 in the form of nanocrystals and mesoporous particles also has capacitive surface storage (involving both faradic and non-faradic or pseudocapacitive processes).[2,10]

Sodium may be an alternative to lithium for non-aqueous batteries.[4,11-14] However, the mechanisms of the reactions between TiO_2 and Na have been little explored in the literature. Xiong et al. found that anatase-type TiO_2 cannot support sodium insertion while only amorphous nanotubes with inner diameter larger than 80 nm can support electrochemical cycling with sodium ions.[11] We have reported recently the electrochemical reaction between amorphous nt-TiO_2 and Na and found that the optimization of the electrochemical behaviour depends more critically in sodium cell than in lithium cells on both the experimental conditions for electrochemical cycling (e.g. lower potential limit, current density and electrolyte composition) and nanotube microstructure (e.g. length and diameter).[4]

In this work we study the electrochemical reaction with Na of self-organized anatase nt-TiO_2 of high aspect ratio and, for this purpose, galvanostatic cycling, cyclic voltammetry, XRD, NMR and impedance spectra are used. To obtain long nanotubes with a wide central cavity, high potential (100 V) voltages were used for the anodization process. The microstructure of the anatase nanotubes is examined by using XRD, SEM and TEM. The faradic and psedocapacitive contribution of the battery are

unfolded.

2. Experimental

2.1 Synthesis and preparation of materials

Self-organized titania nanotubes (nt-TiO_2) were prepared by anodization at 100 V of a Ti foil with 0.127 mm of thickness and using different anodization times (60 or 120 min). The electrolyte solution was ethylene glycol/water (92/8 vol.) mixture containing 0.3 wt % of NH_4F. The counter electrode was a platinum wire.

To obtain anatase phase nanotubes (anatase nt-TiO_2), the previously obtained amorphous nt-TiO_2 were annealed at 550°C in air atmosphere during 2 h.

2.2 Structural and morphological characterization

X-ray diffraction (XRD) patterns were recorded in a Siemens D5000 instrument with CuKα radiation and indexed using the Celref V3 program. Scanning electron microscopy (SEM) images were obtained using a JSM6300 instrument with a secondary electron detector. Transmission electron microscopy (TEM) was performed using a JEOL model JEM2010. To prepare the specimens for TEM examination, the titania nanotube film was scraped from the titanium substrate, the obtained powder was dispersed in ethanol by sonication, and the resulting dispersion was dripped onto the Formvar grid.

The magic angle nuclear magnetic (MAS NMR) spectra of Na-23 were recorded in a Bruker Avance 400 WB instrument at room temperature, using 13 kHz of spin rate, and applying a single pulse sequence of 1.1 μs and a relaxation time of 1 s. The reference was a NaCl aqueous solution (δ= 0 ppm). Prior to record the spectra, the electrodes were recuperated from sodium electrochemical cells, washed with diethylcarbonate solvent in the dry box and dried under dynamic vacuum, to avoid irreversible reactions with air and moisture.

2.3 Electrochemical tests

The electrochemical experiments were carried out in Swagelok-type cells using a VMP instrument. The electrochemical behaviour in sodium cells was studied using a piece of Na like negative electrode and the electrolyte solution was 1 M $NaPF_6$ in ethylenecarbonate: diethylcarbonate =1:1, also containing a small amount (1 wt%) of vinylene carbonate. The positive electrode was a piece of anodized titanium, involving self-organized nt-TiO_2 film supported on the Ti substrate. Binder was not used. The capacity values are referred to the geometrical area of the electrode (in mAh cm^{-2} units) or to the mass of titania (mAh g^{-1} units). To determine the mass of the electrode (about 0.30 mg), the nanotubes were mechanically scraped from the substrate and weighed.

The ac impedance spectra were recorded using three-electrode cell with T-configuration in the VMP instrument.

3. Results and discussion

3.1 Structure and morphology

The anodization process of titanium foil to produce titania nanotubes involves that the reflections of metallic Ti (s.g. P63/mmc) gradually disappear. For 60 min of anodization, the reflections of the metallic Ti substrate and anatase coexist (not shown). Prior to annealing, the titania nanotubes obtained by anodization of titanium are XRD-amorphous (not shown). After annealing at 550°C the titania nanotubes crystallize to the anatase structure (JCPDS reference card number. 21-1272) (Fig. 1). The average grain size of anatase nt-TiO_2 is Lc=18 nm, obtained from the broadening of the Bragg reflections and the Scherrer equation ($Lc= (0.94\lambda)/(\beta\cos\theta)$).

In order to study the preferred orientation of anatase nt-TiO_2, XRD patterns were recorded (Fig. 1) for (a) self-organized nt-TiO_2 with the nanotube axis oriented perpendicularly to the XRD sample-holder surface and (b) powdered nt-TiO_2 previously scratched from the Ti substrate and mixed with silicone grease to avoid any preferred orientation. The results clearly show that the oriented anatase nt-TiO_2 film exhibits a more intense (004) reflection. Thus, the nanotube axis preferentially runs perpendicular to the (004) plane. These results are in good agreement with the calculations about the structure and strain energies of anatase nanotube obtained by Ferrari et al, that found that an anatase (001) layer would stabilize the rolling of the corresponding nanotube.[15] Brezensinski et al. also found crystallographically orientated nanocrystals in mesoporous anatase thin films using WAXD.[2] Since the anatase nanotubes are self-organized and form a thin film with a certain crystalline orientation on the Ti substrate, this material is analogous to an epitaxial film.

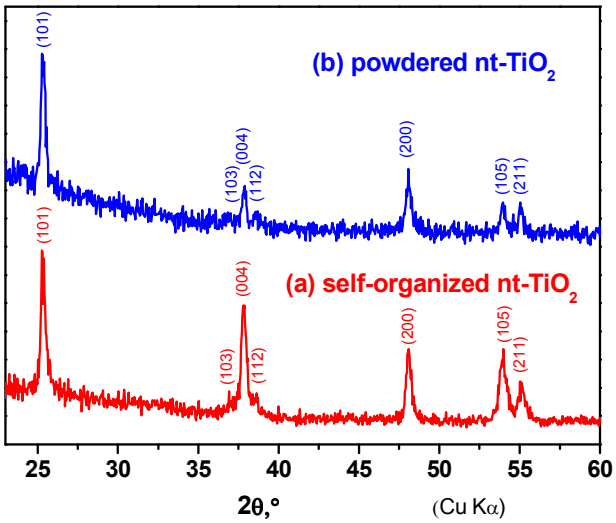

Fig.1 XRD patterns of anatase nanotubes (100 V-120 min-550°C) for (a) self-organized nt-TiO_2 film with the nanotube axis oriented perpendicular to the Ti substrate and (b) non-oriented nt-TiO_2 (powder freed from the Ti substrate and mixed with silicone grease to avoid preferred orientation). The Miller indexes are indicated.

On the other hand, the preferred orientation of nt-TiO_2 can influence on the diffusion of alkali metals into the empty zigzag channels of the anatase framework, the surface properties and the resulting capacity (insertion and surface capacity) in lithium and sodium cells.[16]

The morphology and microstructure was studied using TEM and SEM (Fig. 2). According to the SEM results, the average length of the nanotubes obtained at 100 V is ca. 38 μm after 60 min and ca. 67 μm after 120 min. The length of the nanotubes

may be optimum to achieve high areal capacity in batteries.

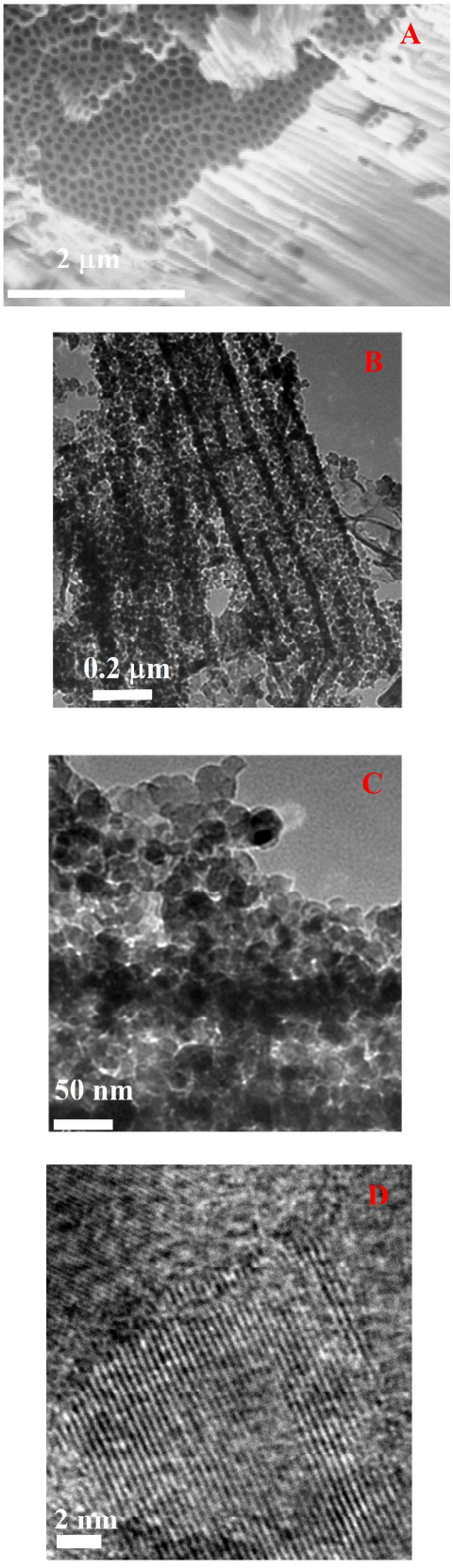

Fig.2 Selected SEM (A) and TEM (B-D) micrographs for anatase nt-TiO_2 obtained by anodization of titanium at 100 V.

The self-arrangement of amorphous nt-TiO_2 retains its morphology and the pores do not fuse and remain open after crystallization to anatase phase, according to the TEM images (Fig. 2). As due the high anodization voltage, the inner diameter (or pore size) is about 92 nm and the wall thickness is about 30 nm. The walls of the nanotubes are composed of grains with size of around 10-30 nm, which is good agreement with the average grain size obtained from the XRD line broadening. Fringes can be observed in the HRTM image. It is worth to note that the thin walls can more easily accommodate expansion or contraction during the alkali metal insertion/deinsertion process.[17]

3.6 Electrochemical reaction of anatase nt-TiO_2 with Na

On the contrary to lithium, the electrochemical reaction of anatase nt-TiO_2 with sodium does not give any extended and reversible plateau in the potential-capacity curve (Figs. 3 and 4). Only a pseudoplateu is observed at about 1.4-1.2 V in the discharge process and about 1.6-2.0 V in the charge process (Fig. 3A). Consequently, first-order structural transitions do not happen reversibly for anatase in sodium cell, on the contrary to lithium.[9] In addition, the XRD reflections of anatase are observed after its reaction with sodium (not shown) and, consequently, we can conclude that the structure of self-organized nt-TiO_2 is preserved even at 0.0 V vs. Na^+/Na. However, the XRD results cannot discard a partial reduction of the titanium ions, for example due to accommodation of sodium in the surface of the anatase nanotubes.

For the nanotubes with average length L= 38 μm, and using 1.0 V or 0.5 V of lower potential limit (Fig. 3), the resulting areal capacity values are not very high (around 0.10-0.25 mAh cm^{-2}). The cycling stability is good (Fig. 3B). The decrease of the potential limit from 1.0 to 0.5 V involves the decrease of the initial coulombic efficiency. In other words, more irreversible reactions are taking place for the first cycle to 0.5 V than 1.0 V.

The longer nanotubes (obtained by anodization during 120 min and length L=67 μm) exhibit higher areal capacity values (Fig. 4). For these electrode materials, it was possible to scrap the nt-TiO_2 film form the Ti substrate, to weigh the active material mass and then to give the gravimetric capacity values. In addition, we have tested the cycling behaviour at different kinetics. At slow kinetics (0.05 mA cm^{-2} of current density) the reversible capacity is around 100-200 mAh g^{-1}. At very high kinetics (5 mA cm^{-2}) the reversible capacity is only about 15 mAh g^{-1}, but the capacity is recuperated when the current density is decreased again (125 mAh g^{-1} or 1.1 mAh cm^{-2} after 100 cycles). For the sake of comparison with other electrode materials, we can note that Rudola et al. reported values of about 70-180 mAh/g for $Na_2Ti_3O_7$,[17] and Xiong et al found around 80-140 mAh g^{-1} for amorphous nt-TiO_2 in sodium cells during the first fifteen cycles.[11] It is worth recalling that here we are using self-organized anatase nanotubes with certain preferred orientation and this fact can affect to the lithium diffusivity and reactivity of TiO_2.

In order to achieve higher capacity values, we have studied the electrochemical behaviour using lower values of potential limit. However, if we decrease the lower potential limit, an irreversible and much extended plateau is observed at around 0.17 V (Fig. 5A). For galvanostatic experiments at low current density (0.05 mA cm^{-2}) the plateau at ca. 0.17 V was apparently endless and, consequently, it was limited by the imposed time. This

irreversible low-voltage plateau only is observed for anatase nt-TiO_2 in sodium cell, neither for amorphous nt-TiO_2 nor for lithium cell, and is ascribed to irreversible reactions such as extended electrolyte solution decomposition in the surface of anatase nt-TiO_2. More probably, the crystallites orientation in the anatase nanotubes can contribute to enhance its reactivity vs. sodium electrolyte solution. Apparently, the surface exposing the crystallographic planes perpendicular to the (004) plane (those with with l=0) would be more reactive. On the other hand, the decomposition of water trapped in the longer nanotubes (120 min of anodization) also may contribute to the irreversible faradic reactions. Consequently, to decrease irreversibility and for effective using anatase nt-TiO_2 in sodium ion batteries, the length of the anatase nanotubes and the lower potential limit should be limited.

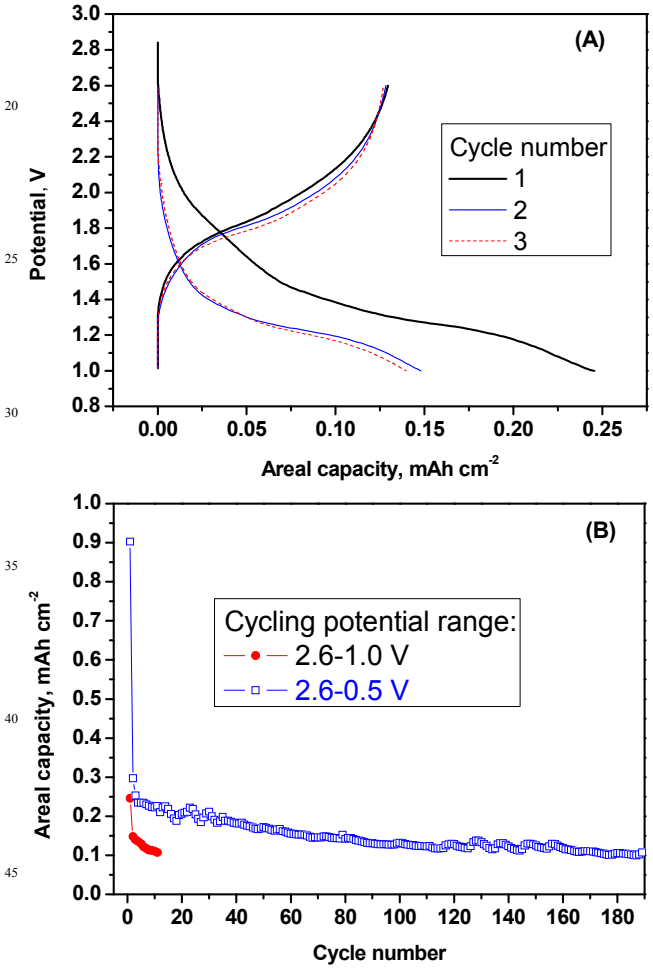

Fig. 3 Electrochemical results for the reaction between anatase nt-TiO_2 (100 V-60 min-550°C) and sodium. (A) Potential-capacity curves for the first three cycles in the range of 2.6-1.0 V. (B) Discharge capacity as a function of cycle number for two different lower potential limits (0.5 and 1.0 V). Imposed current density= 0.1 mA cm^{-2}.

In a try to further optimize the electrochemical cycling, we have found that higher areal capacity values are achieved when the anatase is discharged to about 0.5 V of potential limit during the first few cycles and after further cycles the cut-off potential is decreased to 0.20 V, in comparison with directly cycling to 0.25 V of limit (Fig. 5). In this case, the observed reversible capacity values are very high (up to 400 mAh g^{-1}) but the capacity retention is poor.

As a conclusion, the values of gravimetric and areal capacity are strongly affected by the experimental cycling conditions, and particularly the lower potential limit should be over ca. 0.3 V to avoid extended irreversible reactions and low coulombic efficiency.

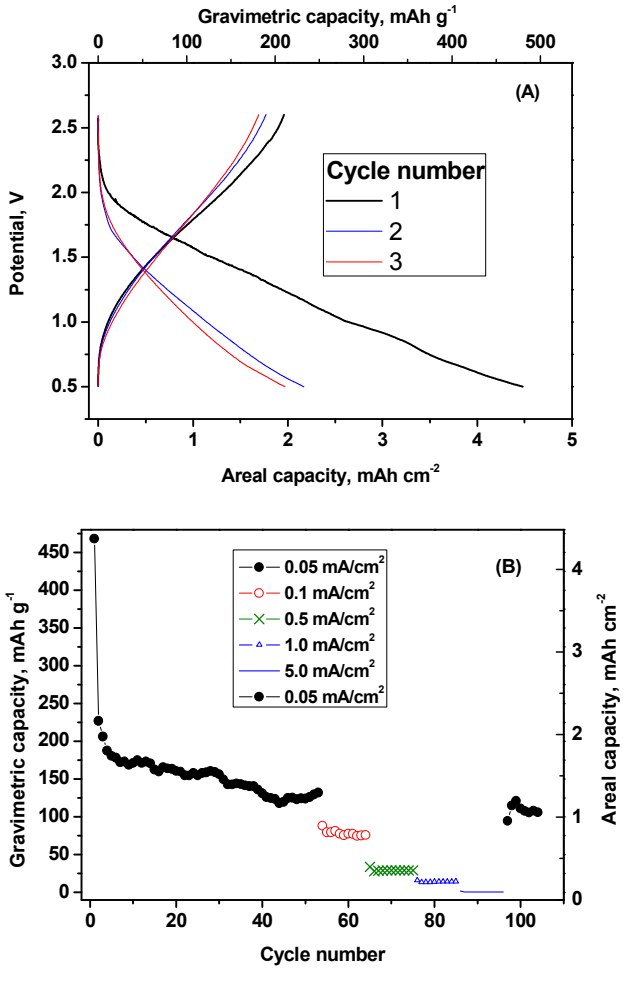

Fig. 4 Electrochemical results for the reaction between anatase nt-TiO_2 (100 V-120 min-550°C) and sodium in the potential range of 2.6-0.5 V. (A) Potential-capacity curves for the first three cycles and using 0.05 mA cm^{-2} of current density. (B) Discharge capacity as a function of cycle number for variable current density.

As a way to understand the origin of the capacity when anatase nt-TiO_2 reacts with sodium, the b-values were obtained from the cyclic voltammograms recorded at several rates (Fig. 6), by first time in this work, and using procedures described in the literature.[2,11,18] The parameter b is directly determined from the slope of the plot of log i versus log v, where v is the sweep rate and i is the current ($i = av^b$). Generally, if the b equals one, a surface redox reaction involving non-diffusion-controlled

processes is expected; meanwhile for the ideal diffusion-controlled faradaic process, the slope b equals 0.5 and satisfies Cottrell's equation ($i=av^{0.5}$).

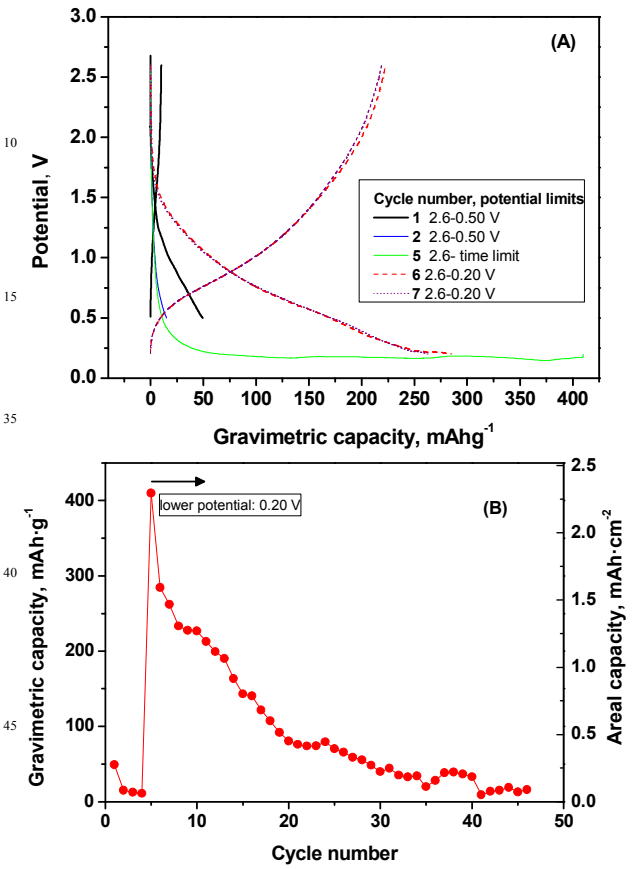

Fig. 5 Electrochemical results for the reaction between anatase nt-TiO_2 (100 V- 120 min-550°C) and sodium under different cycling conditions, particularly the lower potential limit. (A) Potential-capacity curves for the cycle number 1, 2, 5, 6 and 7, and using different potential limits. (B) Capacity as a function of cycle number obtained from (A). Current density: 0.05 mA cm^{-2}.

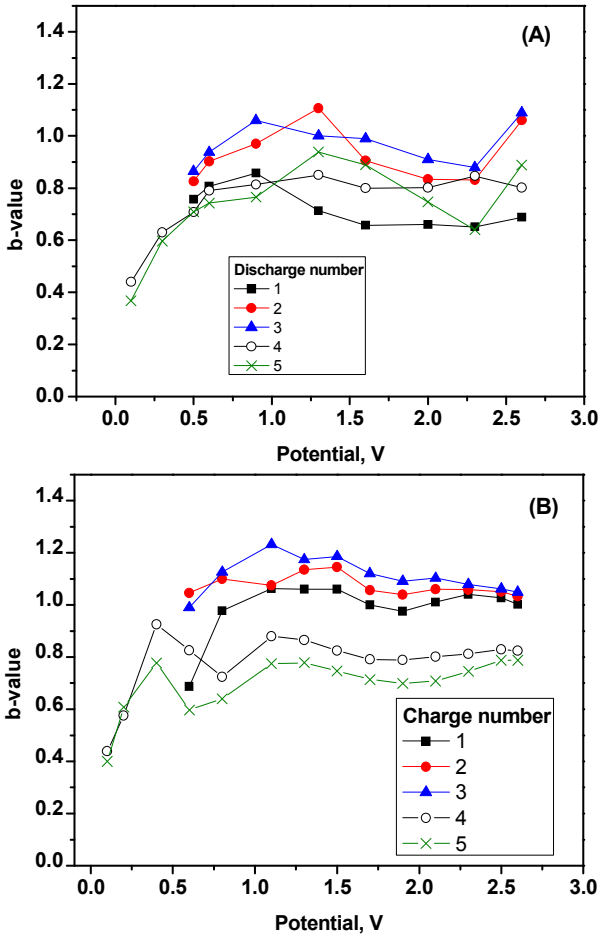

Fig. 6 b-value for anatase nt-TiO_2 (100 V-120 min-550°C) in sodium cell for discharge (A) and charge (B). For the cycle number one to three each battery was discharged to 0.5 V, and for the cycle number four and five the cut-off potential was 0.01 V.

In these experiments, during the first three discharge-charge cycles, the cut-off potential limit was 0.5 V, and then was decreased to 0.01 V. During the first discharge process the resulting b-value is ranged between ca. 0.7 and 0.8. Since the b-values obtained in the second and third cycles in the potential range between 0.5 and 2.5 V are near 1.0, we assume that the reaction is mainly due to reversible accommodation of sodium in the surface of anatase nt-TiO_2 (surface pseudocapacitive process or non-diffusion controlled process). Probably the increase of the b-value from cycle one to three is due to decrease of the contribution of electrolyte decomposition (faradic processes). The b-values during the charge are also about 1.0. After the first three cycles, the potential limit was decreased from 0.5 to 0.0 V and it results that in the region about 0.1-0.3 V the b-value is near to 0.5 (faradic-type processes) for both discharge and charge processes. According to the resulting b-values, both electrolyte decomposition and sodium insertion into TiO_2 may contribute to the faradic processes that take place below ca. 0.3 V. Consequently, it seems that in the first discharge certain passivation processes take place and this passivation is effective for cycling over ca. 0.3 V but nor for cycling at voltages below ca. 0.3 V. The irreversible processes are not accompanied by passivation and formation of stable films below ca. 0.3 V. These results are in quite good agreement with the galvanostatic cycling results (Fig. 3 and 4). Similarly, Xiong et al. found that the b-value for amorphous nt-Na_xTiO_2 tends to decreases from 1.4 V to 0.5 V.[11]

The irreversible faradic processes below 0.25 V seem to be a property enhanced for the self-organized anatase nanotubes due to its crystallographic orientation and the reactivity of the crystallites surface against the sodium-based electrolyte solution.

In comparison with the b-values corresponding to the intercalation lithium into anatase reported by Brezkinski et al lithium,[2] the true intercalation of sodium is discarded here.

3.6 Nuclear magnetic resonance

While XRD reveals information on the crystalline structure, NMR can provides information on the local environment of the studied nucleus.[19, 20] The observed ^{23}Na MAS NMR spectra for anatase nt-Na_xTiO_2 electrodes recuperated from sodium cells (Fig. 7) are complicated by the second-order quadrupole broadening and are quite similar to the spectra for mesoporous titanium oxide reported by Lo et al.[20] Besides the spinning side bands, we can see that the spectra in the partially discharged (1.0 V), totally discharged (0.0 V) and recharged (2.6 V) states are different. All the spectra exhibit a sharp peak at about 5 ppm and a broadened resonance centered at about – 11 ppm. The narrow peak placed 5 ppm has small quadrupolar interactions and most probably is due to sodium ions with high mobility in compounds formed by irreversible electrolyte decomposition at the surface of anatase nt-TiO_2. Tentatively, the broadened resonance centred at about -11 ppm may be due to sodium ions with reduced mobility that are placed in the surface of anatase nt-TiO_2 (or in other words, in the walls of the nanotubes). Thus, the relative intensity of the broadened resonance reversibly increases when the cell is discharged (reaction with sodium). Since, the shift of the broader resonance is not very large, a true insertion of the sodium ions into the anatase framework is discarded because strong paramagnetic interactions Na^+/Ti^{3+} ions would not be established. Consequently, the electrochemical reaction to accommodate sodium mainly would take place in the surface of nt-TiO_2.

Investigations of ^{23}Na NMR of sodium-reduced mesoporous titanium oxide also found a sharp peak near 0 ppm and a broadened resonace at about – 15 ppm.[20]

The NMR results agree quite well with the b-values and strongly suggest that the accommodation of sodium in anatase nt-TiO_2 mainly takes place through pseudocapacitive behaviour (surface processes). These results are in good agreement with the conclusions reported by Xiong et al.[11]

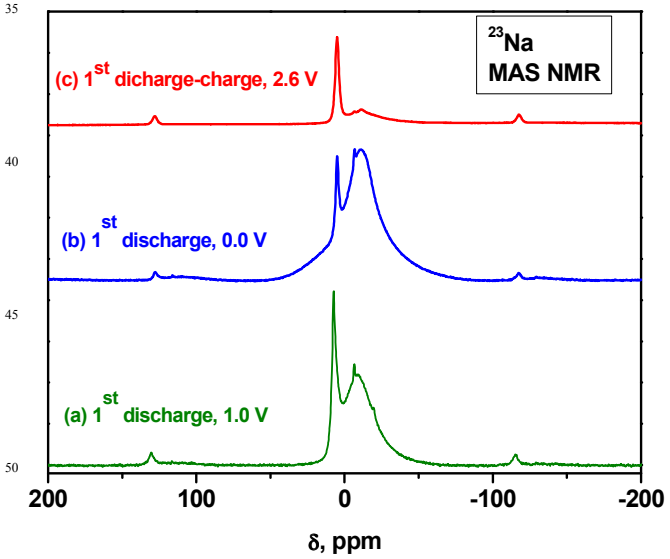

Fig. 7 ^{23}Na MAS NMR spectra for anatase nt-TiO_2 (100 V, 120 min, 550°C) electrodes (a) at 1.0 V vs. sodium (partial first discharge), (b) at 0.01 V vs. sodium (whole first discharge) and (c) at 2.6 V vs. sodium (first discharge-charge cycle).

3.6 Impedance spectroscopy

In order to further study the interface properties of anatase nt-TiO_2 in sodium non-aqueous cells, ac impedance spectra were recorded (Fig. 8). During the the first discharge process from 2.8 V (initial open circuit voltage) to 0.01 V (whole discharge state), a depressed semicircle emerges and its size increases when the potential decreases (Fig. 8A). This fact is due to the surface film formation (surface resistance at high frequencies) and reaction with sodium (charge transfer resistance at intermediate frequencies). The depressed semicircles are typical of porous samples.[21] The contribution of several depressed semicircles cannot be separately distinguished at the initial voltage (2.8 V). The sloped line at very low frequencies is due to sodium diffusion. The spectrum obtained at the end of the first discharge was fitted with the following equivalent circuit: $[R_e(R_{sl}Q_{sl})(R_{ct}W)Q_{ct}]$. The resulting surface layer resistance is R_{sl}= 6.3 Ohm, and the charge transfer resistance is R_{ct}=76.5 Ohm.

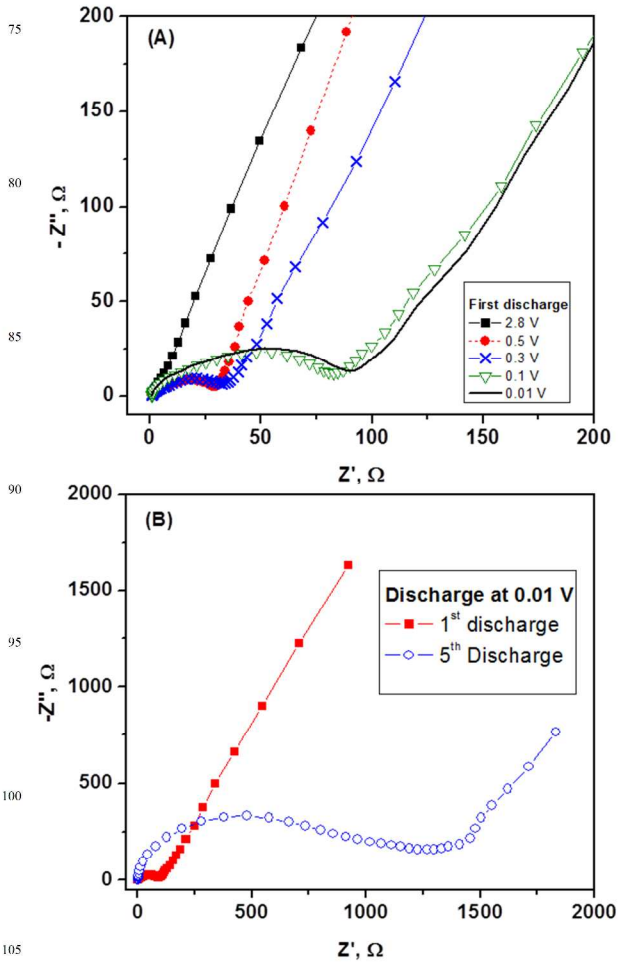

Fig. 8 Impedance spectra for anatase nt-TiO_2 (100 V-120 min-550°C) in sodium cell measured at selected states of the first discharge (A), and at 0.01V for the first and fith discharge (B). Imposed discharge current density: 0.05 mA/cm^2.

From the first to the fifth cycle (Fig. 8B), the size of the depressed semicircles in the discharge state increases, the spectrum becomes more complex, and the impedance rises (in the order of 1 kΩ), as due to electrolyte decomposition processes.

These results confirm our discussion about the obtained b-value and NMR spectra and the occurrence of irreversible redox processes near 0.0 V. Consequently, the composition of the electrolyte solution should be further optimized. Another possible solution may be the modification of the surface properties of anatase nt-TiO_2 by making a protective coating or by optimization of the anodization process and morphology of the nanotubes.

3.6 Further improvement of the electrochemical performance

In order to improve the electrochemical performance of self-organized anatase nt-TiO_2, we have followed a new strategy: the voltage for anodization of Ti was linearly changed with time during the anodization process. Thus, after several tests, we have found a net improvement of the electrochemical cycling when the anodization voltage is increased from 20 to 100 V during 120 min (ΔV_{anod} 20-100 V), while the anodization time and other parameters are not changed in comparison with the anodization process under fixed voltage.

The capacity tends to increase from cycle number 25 (about 100-120 mAh g^{-1}) to about 260 cycle number (220 mAh g^{-1}), and after this is nearly stable (Fig. 9). After 800 cycles, the gravimetric capacity is ca. 190 $mAhg^{-1}$ (using a rate of 1C, or about 1 h for one charge). The reason for such as great improvement of the electrochemical properties is not still completely elucidated. Irrespectively of the excellent cyclability and high gravimetric capacity values, the resulting areal capacity values (about 0.1 mAh cm^{-2}) are lower in comparison with samples obtained at fixed voltage of anodization.

Probably, the resulting modification of the electrochemical properties is due to changes of the morphology and surface properties of the nanotubes. The preliminary results show that, using a 20-100 V of anodization voltage, the inner diameter of the nanotubes is increased (ca.130 nm) and their length is decreased (ca. 6 μm). The total diameter of the nanotubes is also increased u to around 200 nm. Thus, the larger nanotube diameter makes easier the reaction with sodium, while the shorter nanotube length decreases the areal capacity and probably improves the cycling stability. Another possible effect of the variable anodization potential may be that the initial low voltage (20 V) perhaps would allow the formation of a more stable nanotube surface, while the last high voltage (100 V) creates the wider nanotube mouth.

The average operation voltage is about 1.3-1.0 V, depending on the cycle number (Fig. 9A). The high average voltage can be an advantage to the safety of the battery. It is observed that the shape of the potential-capacity curves is modified when the electrochemical cycling progresses. The electrochemical results strongly suggest that an activation process of the electrode material is taking place during the first ca. 50 cycles. The relaxation time periods that were imposed (Fig. 9) also may contribute to create a more stable electrode.

The reason for such as good improvement of the electrochemical behaviour of the anatase nanotubes in sodium cells should be further studied in future studies. The excellent cycling ability and the gravimetric capacity values that we report here are rather comparable with the achievements very recently published by Wu et al. using anatase nanopowder.[22] It is worth to remember that in our case we are using a special type of electrode morphology (self-organized nanotubes which are free of binder and carbon additives) which is particularly more useful for microbatteries. In addition, our anatase nanotubes show preferred crystallographic orientation. On the other hand, probably the composition of the electrolyte solution also may be improved.

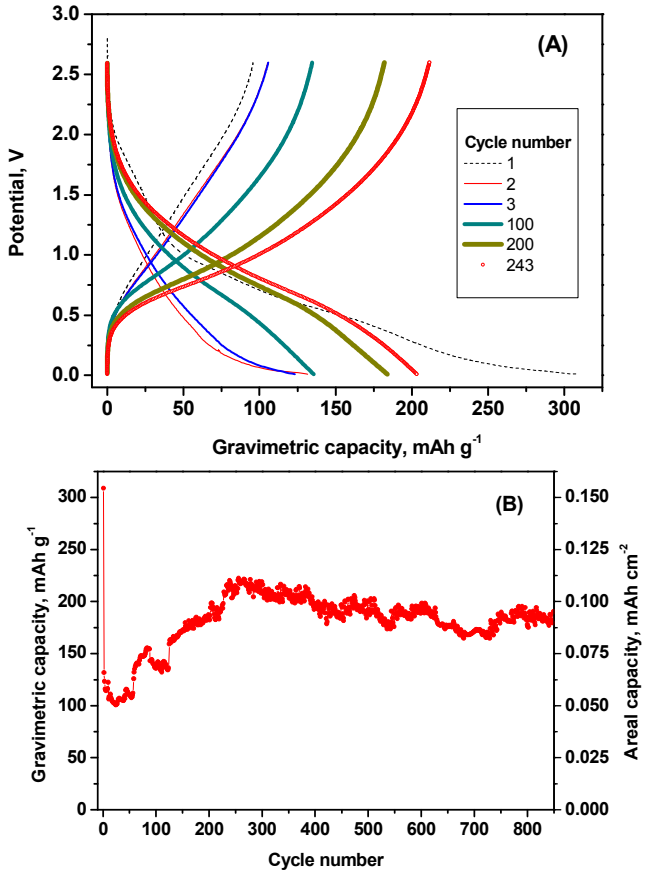

Fig 9 Electrochemical results for the reaction between anatase nt-TiO_2 (20 to 100 V- 120 min-550°C) and sodium. (A) Potential-capacity curves for the cycle number 1, 2, 3, 100, 200 and 243. (B) Capacity as a function of cycle number. Current density: 0.1 mA cm^{-2}. Potential limits: 0.0-2.6 V. The cell was allowed to relax after the cycle number 58 and 125.

4. Conclusions

The walls of self-arranged anatase nt-TiO_2 are composed of nanocrystals with certain preferred orientation. The structure of self-organized anatase nt-TiO_2 is preserved after its electrochemical reaction with sodium. The values of the b-parameter as function of potential for anatase nt-TiO_2 suggest that the contribution of the accommodation of sodium in the surface of anatase nt-TiO_2 in the potential range of 0.5-2.6 V is more important in sodium cell than in lithium cell. At least two types of sodium are found in the ^{23}Na NMR spectra for anatase nt-Na_xTiO_2, and the reversible accommodation of sodium in anatase surface (or nanotubes walls) is inferred from the spectra. It seems that anatase nt-TiO_2 is suitable for cycling in sodium batteries only in the region over ca. 0.3 V. This voltage can be suitable for certain applications. Further optimization of the electrolyte, surface properties and electrochemical cycling conditions may render this electrode material more suitable for high-energy sodium ion batteries.

The anodization under variable voltage renders nanotubes with

excellent cycling behaviour (about 190 mAh g^{-1} after 800 cycles). The reason for this improvement should be further studied, but our preliminary studies suggest that this fact is due to the morphology of the nanotubes, particularly the larger diameter.

Acknowledgements

The authors are indebted to MEC-MAT2011-22753 and *Junta de Andalucía* (FQM288). GOJ is indebted to *Ramón y Cajal* Program.

Notes and references

[a] *Laboratorio de Química Inorgánica, Universidad de Córdoba, Edificio Marie Curie (C3), planta 1,Campus de Rabanales, 14071 Córdoba, Spain. Fax: 34 957218621; Tel: 34 957218637; E-mail: iq2alror@uco.es*

† Electronic Supplementary Information (ESI) available: [details of any supplementary information available should be included here]. See DOI: 10.1039/b000000x/

‡ Footnotes should appear here. These might include comments relevant to but not central to the matter under discussion, limited experimental and spectral data, and crystallographic data.

1 D. Deng, M. G. Kim, J. Y. Lee and J. Cho, *J. Energy Environ. Sci.*, 2009, **2**, 818; Z. Bi, M. P. Paranthaman, P. A. Menchhofer, R. R. Dehoff, C. A. Bridges, M.. Chi, B. Guo, X. G. Sun and S. Dai, *J. Power Sources*, 2013, **222**, 461; H. Xiong, H. Ildirim, E. V. Shevchenko, V. B. Prakapenka, B. Koo, M. D. Slater, M. Balasubramanian, S. K. R. S. Sankaranarayanan, J. P. Greeley, S. Tepavcevic, N. M. Dimitrijevic, P. Podsiadlo, C. S. Johnson and T. J. Rajh, *J. Phys. Chem. C*, 2012, **116**, 3181;V. Subramanian, A. Karki, K. I. Gnanasekar, F. P. Eddy and B. Rambabu, *J. Power Sources*, 2006, **159**, 186; S. W. Oh, S. H. Park and Y. K. Sun, *J. Power Sources*, 2006, **161**, 1314.

2 T. Brezesinski, J. Wang, J. Polleux, B. Dunn and S. H. J. Tolbert, *J. Am. Chem. Soc.*, 2009, **131**, 1802.

3 J. R. González, R. Alcántara, F. Nacimiento, F. G. F. Ortiz, J. L. Tirado, E. Zhecheva and R. Stoyanova, *J. Phys. Chem. C*, 2012, **116**, 20182.

4 J. R. González, R. Alcántara, G. F. Ortiz, F. Nacimiento and J. L. Tirado, *J. Electrochem. Soc.*, 2013, **160**, A1390.

5 A. Valota, D. J. LeClere, P. Skeldon, M. Curioni, T. Hashimoto, S. Berger, J. Kunze, P. Schmuki and G. E. Thompson, *Electrochim. Acta*, 2009, **54**, 4321.

6 S. Y. Huang, L. Kavan, I. Exnar and M. Grätzel, *J. Electrochem. Soc.*, 1995, **142**, L142.

7 F. Bonino, L. Busani, M. Lazzari, M. Manstretta, B. Rivolta and, B. Scrosati, *J. Power Sources*, 1981, **6**, 261.

8 T. Ohzuku, T. Kodama and T. Hirai, *J. Power Sources*, 1985, **14**, 153.

9 L. J. Hardwick, M. Holzapfel, P. Novák, L. Dupont and E. Baudrin, *Electrochim. Acta*, 2007, **52**, 5357; M. Wagemaker, W. J. H. Borghols, F. M. Mulder, J. Am. Chem. Soc. 2007, 129, 4323; U. Lafont, D. Carta, G. Mountjoy, A. Chadwick and E. M. Kelder, *J. Phys. Chem. C*, 2010, **114**, 1372; V. Gentili, S. Brutti, L. J. Hardwick, A. R. Armstrong, S. Panero and P. G. Bruce, *Chem. Mater.,* 2012, **24**, 4468.

10 W. J. H. Borghols, D. Luetzenkirchen-Hecht, U. Haake, W. Chan, U. Lafont, E. M. Kelder, E. R. H. van Eck, A. P. M. Kentgens, F. M. Mulder and M. Wagemaker, *J. Electrochem. Soc.*, 2010, **157**, A582.

11 H. Xiong, M. D. Slater, M. Balasubramanian, C. S. Johnson and T. Rajh, *J. Phys. Chem. Lett.*, 2011, **2**, 2560.

12 V. Palomares, M. Casas-Cabanas, E. Castillo-Martinez, M. H. Han and T. Rojo, *Energy Environ. Sci.*, 2013, **6**, 2312.

13 J.R. González, F. Nacimiento, R. Alcántara, G. F. Ortiz and J. L. Tirado, *CrystEngComm*, 2013, **15**, 9196.

14 Y. Xu, E. M. Lotfabad, H. Wang, B. Farbod, Z. Xu, A. Kohandeghan and D. Mitlin, Chem. Commun., 2013, **49**, 8973.

15 A. M. Ferrari, D. Szieberth, C. M. Zicovich-Wilson and R. Demichelis, *J. Phys. Chem. Lett.*, 2010, **1**, 2854.

16 G. Nuspl, K. Yoshizawa and T. Yamabe, *J. Mater. Chem.*, 1997, **7**, 2529.

17 A. Rudola, K. Saravanan, C. W. Mason and P. Balaya, *J. Mater Chem. A*, 2013, **1**, 2653; P. Senguttuvan, G. Rousse, V. Seznec, J. M. Tarascon and M. Rosa Palacín, *Chem. Mater*., 2011, **23**, 4109.

18 J. Wang, J. Polleux, J. Lim and B. Dunn, *J. Phys. Chem. C*, 2007, **111**, 14925; M. C. López, G. F. Ortiz, P. Lavela, R. Alcántara and J. L. Tirado, *ACS Sustainable Chem. Eng.*, 2013, **1**, 46.

19 R. Alcántara, P. Lavela, G. F. Ortiz and J. L. Tirado, *Electrochem. Solid-State Lett.*, 2005, **8**, A222.

20 A. Y. H. Lo, R. W. Schurko, M. Vettraino, B. O. Skadtchenko, M. Trudeau and D. M. Antonelli, *Inorg. Chem.*, 2006, **45**, 1828.

21 M. Dubois and D. Billaud, *Electrochim. Acta*, 2002, **47**, 4459.

22 L. Wu, D. Buchholz, D. Bresser, L. G. Chagas and S. Passerini, *J. Power Sources*, 2014, **251**, 379.

Anatase nanotubes showing preferred orientation and high capacity versus sodium and during many electrochemical cycles.